

# Bridging Traditional and Machine Learning-Based Algorithms for Solving Partial Differential Equations: The Random Feature Method

Weinan E

Peking University

Beijing, 2022

## Collaborators

- ▶ Jingrun Chen, USTC
- ▶ Xurong Chi, USTC
- ▶ Zhouwang Yang, USTC



## Example: Two-dimensional Poisson Equation

1. Strong form: Find  $u(x, y) \in C^2(\Omega)$ , s.t.

$$\begin{aligned} -\Delta u(x, y) &= f(x, y), & \text{in } \Omega \\ u(x, y) &= 0, & \text{on } \partial\Omega \end{aligned}$$

or

$$\min_{u(x,y) \in H_0^1(\Omega)} \int_{\Omega} (\Delta u + f)^2 \, dx dy$$

2. Weak form: Find  $u(x, y) \in H_0^1(\Omega)$ , s.t.

$$\int_{\Omega} \nabla u \cdot \nabla v \, dx dy = \int_{\Omega} f v \, dx dy, \quad \forall v \in H_0^1(\Omega)$$

3. Variational form :

$$\min_{u(x,y) \in H_0^1(\Omega)} \int_{\Omega} \left( \frac{1}{2} |\nabla u|^2 - fu \right) \, dx dy$$

# Numerical algorithms

- ▶ Low computational cost
- ▶ Low human cost
- ▶ Robustness and generality

An incomplete list of some of the difficulties we still encounter

- ▶ Problems with complex geometry: Stokes flow in porous media
- ▶ Kinetic equations: Direct simulation Monte Carlo algorithm
- ▶ Multi-scale problems

# Outline

Traditional Algorithms

Machine Learning-based Algorithms  $M \neq N$

A Bridge Between Traditional and Machine-learning Algorithms

# Traditional Algorithms

- ▶ Strong form: Finite Difference Method, Spectral Collocation Method, Least Square Method
- ▶ Variational form: Ritz Method
- ▶ Weak form: Finite Element Method, Spectral (Galerkin) Method, Spectral Element Method, Mesh-free Method, etc

# Finite Difference Method

- ▶ Discretization of equation  $\rightarrow$  grid points (collocation points)

$$-\Delta u(x_{i,j}) = f(x_{i,j})$$

- ▶ Discretization of operator  $\rightarrow$  finite difference

$$\frac{4u_{i,j} - u_{i-1,j} - u_{i+1,j} - u_{i,j-1} - u_{i,j+1}}{h^2} = f_{i,j}$$

- ▶ Boundary condition

$$u_{1,j} = u_{m,j} = u_{i,1} = u_{i,n} = 0$$

- ▶ Total number of conditions = total number of unknowns

Simple, but not easy to handle complex geometries

# Spectral Collocation Method

- ▶ Discretization of equation  $\rightarrow$  grid points (collocation points)

$$-\Delta u(x_{i,j}) = f(x_{i,j})$$

- ▶ Approximation space: Linear combinations of global polynomials (Lagrange polynomials, Fourier polynomials, Chebyshev polynomials, etc)

$$u_N(x, y) = \sum_{i,j} \phi_{ij}(x, y) u_{ij}$$

- ▶ Polynomial basis functions need to satisfy boundary conditions

Spectral accuracy, not easy to handle complex geometries

# Ritz Method

- ▶ Approximation space: Linear combinations of global basis functions (Polynomials, Trigonometric functions, etc)

$$u_N(x, y) = \sum_{i,j} \phi_{ij}(x, y) u_{ij}$$

- ▶ Basis functions need to satisfy boundary conditions
- ▶ Variational problem: Numerical integration

$$u_N(x, y) = \arg \min_{v_N(x,y) \in H_0^1(\Omega)} \int_{\Omega} \left( \frac{1}{2} |\nabla v_N|^2 - f v_N \right) dx dy$$

Not easy to handle complex geometries (boundary conditions and numerical integration)

# Finite Element Method

- ▶ Mesh generation: Tedious and time-consuming ( $\sim 70\%$  for solving a PDE problem)
- ▶ Basis functions: linear combinations of local piecewise polynomials

$$u_N(x, y) = \sum_{i,j} \phi_{ij}(x, y) u_{ij}$$

- ▶ Weak form

$$\int_{\Omega} \nabla u_N \cdot \nabla v \, dx \, dy = \int_{\Omega} f v \, dx \, dy, \quad \forall v \in V_N$$

- ▶ Boundary conditions can be enforced easily

Simple, easy to handle complex geometries, but generating the mesh is not easy



# Spectral (Galerkin) Method

- ▶ Approximation space: Linear combinations of global polynomials

$$u_N(x, y) = \sum_{i,j} \phi_{ij}(x, y) u_{ij}$$

- ▶ Polynomial basis functions need to satisfy boundary conditions
- ▶ Weak form

$$\int_{\Omega} \nabla u_N \cdot \nabla v \, dx \, dy = \int_{\Omega} f v \, dx \, dy, \quad \forall v \in V_N$$

Simple, spectral accuracy, not easy to handle complex regions  
(boundary conditions, numerical integration)

# Spectral Element Method

- ▶ Mesh generation
- ▶ Approximation space: Linear combination of local higher-degree polynomials (Double summation of order index and element index)

$$u_N(x, y) = \sum_{i,j} \phi_{ij}(x, y) u_{ij}$$

- ▶ Boundary conditions can be implemented easily
- ▶ Weak form:

$$\int_{\Omega} \nabla u_N \cdot \nabla v \, dx dy = \int_{\Omega} f v \, dx dy, \quad \forall v \in V_N$$

Spectral accuracy, easy to handle complex geometries  
Mesh generation, boundary conditions and numerical integration  
can be difficult

# Meshfree Method

- ▶ Approximation space: Linear combinations of global and local functions  $u_N(x, y) = \sum_{i,j} \phi_{ij}(x, y) u_{ij}$
- ▶ Boundary conditions are enforced by a penalty term
- ▶ Weak form:

$$\int_{\Omega} \nabla u_N \cdot \nabla v \, dx \, dy = \int_{\Omega} f v \, dx \, dy, \quad \forall v \in V_N$$

Simple, algebraic accuracy, not easy to handle complex geometries (numerical integration)

# Accuracy vs Efficiency

## WHICH METHOD IS BETTER???

- ▶ Strong form: Collocation points
- ▶ Weak form: Numerical integration
- ▶ Approximation space
- ▶ Boundary conditions

Note that we always have  $M = N$ , where

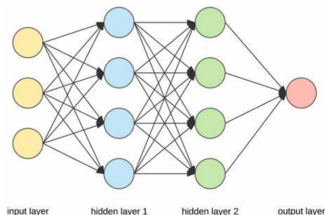
- ▶  $M$  = number of parameters
- ▶  $N$  = number of equations, or collocation points

# Deep Neural Network

A new approximation space

$$u(x, y) = W\sigma(W_2\sigma(W_1\mathbf{x} + b_1) + b_2)$$

How to optimize the parameters  $W$  and  $b$ ?



- ▶ Strong form: Collocation points
- ▶ Variational form: Numerical integration or Monte-Carlo sampling
- ▶ Weak form: Numerical integration or Monte-Carlo sampling

# Components of a machine-learning algorithm

- ▶ Loss function: Strong, variational, weak  
Collocation point, Quadrature or Monte Carlo sampling
- ▶ Approximation space: Deep neural networks
- ▶ Optimization of NN parameters: Stochastic gradient descent method

# Comparison

- ▶ Error sources: approximation, integration, optimization
- ▶ SGD can get a reasonable solution, which is not good enough
- ▶ In high dimension
  - ▶ Traditional methods fail
  - ▶ Deep learning methods work (1% relative error without convergence order)
- ▶ In low dimension  $d \leq 3$ 
  - ▶ Traditional methods typically work well
  - ▶ Deep-learning methods work (1% relative error without convergence order), but have high coding efficiency

# Machine Learning-based Algorithms

- ▶ Variational form: Deep Ritz Method (DRM)<sup>1</sup>
- ▶ Strong form: Deep Galerkin Method (DGM)<sup>2</sup>, Physics-Informed Neural Networks (PINN)<sup>3</sup>
- ▶ Weak form: Weak Adversarial Network (WAN)<sup>4</sup>
- ▶ etc

---

<sup>1</sup>EY2018.

<sup>2</sup>SS2018.

<sup>3</sup>PINN.

<sup>4</sup>Bao.



# Deep Ritz Method

$$\begin{cases} -\Delta u(x) = f(x), & x \in \Omega \\ u(x) = g(x), & x \in \partial\Omega \end{cases}$$

Loss function: Variational form + boundary penalty term

$$I[u] = \int_{\Omega} \left( \frac{1}{2} |\nabla u(x)|^2 - f(x)u(x) \right) dx + \lambda \int_{\partial\Omega} (u(x) - g(x))^2 dx$$

Optimization:

$$\begin{aligned} \theta_{k+1} = & \theta_k - \alpha \nabla_{\theta} \frac{|\Omega|}{N_v} \sum_{i=1}^{N_v} \left[ \frac{1}{2} |\nabla u(x_i)|^2 - f(x_i) u(x_i) \right] \\ & - \lambda \alpha \nabla_{\theta} \frac{|\partial\Omega|}{N_b} \sum_{j=1}^{N_b} [u(y_j) - g(y_j)]^2 \end{aligned}$$

- ▶ Variational form: ReLU converges in general
- ▶ Boundary condition is enforced by penalty term, but the penalty parameter is difficult to tune
- ▶ Loss function can be negative
- ▶  $M \neq N$

# DGM, PINN

$$\partial_t u = \mathcal{L}u, \quad (t, x) \in [0, T] \times \Omega$$

$$u(0, x) = u_0(x), x \in \Omega$$

$$u(t, x) = g(x), \quad (t, x) \in [0, T] \times \partial\Omega$$

Loss function: strong form in the least-squares sense + boundary penalty term

$$L(u) = \|\partial_t u - \mathcal{L}u\|_{2, [0, T] \times \Omega}^2 + \lambda_1 \|u(0, \cdot) - u_0\|_{2, \Omega}^2 \\ + \lambda_2 \|u - g\|_{2, [0, T] \times \partial\Omega}^2$$

- ▶ Strong form: High regularity, and usually ReLU does not converge
- ▶ Boundary condition is enforced by penalty term, but the penalty parameter is difficult to tune
- ▶  $M \neq N$

$$\begin{cases} \langle \mathcal{A}[u], \varphi \rangle \triangleq \int_{\Omega} \left( \sum_{j=1}^d \sum_{i=1}^d a_{ij} \partial_j u \partial_i \varphi + \sum_{i=1}^d b_i \varphi \partial_i u + c u \varphi - f \varphi \right) dx = 0 \\ \mathcal{B}[u] = 0, \quad \text{on } \partial\Omega \end{cases}$$

Loss function: weak form

$$\|\mathcal{A}[u]\|_{op} \triangleq \max \{ \langle \mathcal{A}[u], \varphi \rangle / \|\varphi\|_2 \mid \varphi \in H_0^1, \varphi \neq 0 \}$$

$$\min_{u \in H^1} \|\mathcal{A}[u]\|_{op}^2 \iff \min_{u \in H^1} \max_{\varphi \in H_0^1} |\langle \mathcal{A}[u], \varphi \rangle|^2 / \|\varphi\|_2^2$$

$$L_{\text{int}}(\theta, \eta) \triangleq \log |\langle \mathcal{A}[u_{\theta}], \varphi_{\eta} \rangle|^2 - \log \|\varphi_{\eta}\|_2^2$$

$$L_{\text{bdry}}(\theta) \triangleq (1/N_b) \cdot \sum_{j=1}^{N_b} \left| u_{\theta}(x_b^{(j)}) - g(x_b^{(j)}) \right|^2$$

$$\min_{\theta} \max_{\eta} L(\theta, \eta), \quad \text{where } L(\theta, \eta) \triangleq L_{\text{int}}(\theta, \eta) + \alpha L_{\text{bdry}}(\theta)$$

- ▶ Weak form: ReLU converges in general
- ▶ Boundary conditions require penalty terms
- ▶ Min-max problem: uses GAN to solve and takes longer to optimize
- ▶  $M \neq N$

# Machine Learning-based Algorithms

- ▶ Simple, meshfree, easy to handle complex geometries and boundary conditions
- ▶ The accuracy cannot be improved systematically and the penalty parameters are difficult to tune
- ▶ Training takes a long time and the optimization error is difficult to quantify
- ▶ Low human cost and low application barrier

# Local Extreme Learning Machine<sup>6</sup>

- ▶ Strong form: collocation points
- ▶ Approximation space: domain decomposition + extreme learning machine (only parameters in the output layer optimized)<sup>5</sup>
- ▶ Linear least-squares problem  $M \neq N$
- ▶ Similar to the spectral element method

Spectral accuracy, easy to handle complex geometries

---

<sup>5</sup>huang2006extreme.

<sup>6</sup>dong2021local.

- ▶ Scalar PDE form

$$\begin{cases} \mathcal{L}u(\mathbf{x}) = f(\mathbf{x}), & \text{in } \Omega \\ \mathcal{B}u(\mathbf{x}) = g(\mathbf{x}), & \text{on } \partial\Omega \end{cases}$$

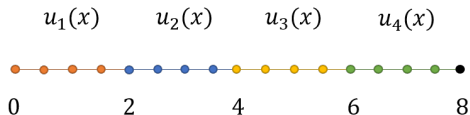
- ▶ Domain decomposition:  $\Omega = \Omega_1 \cup \Omega_2 \cup \dots \cup \Omega_{N_e}$
- ▶ Local neural network is used to represent the solution in each subdomain
- ▶ Continuity conditions of basis functions and derivatives are enforced
- ▶ Main steps in the algorithm:
  - 1 Selecting collocation points in subdomains  $\Omega_s$
  - 2 Evaluating the equations at interior points and boundary/continuity conditions at (sub-)boundary points
  - 3 Solving the least-squares problem



# Illustration

Domain  $[0, 8]$  with  $N = 4$  subdomains

- ▶ Equation at all points
- ▶ Boundary conditions at  $x = 0$  and  $x = 8$
- ▶ Continuity conditions at  $x = 2$ ,  $x = 4$  and  $x = 6$



## Exponential convergence for Helmholtz equation

| N  | $L^\infty$ error | $L^2$ error |
|----|------------------|-------------|
| 4  | 8.76E-2          | 2.31E-2     |
| 8  | 4.06E-7          | 1.20E-7     |
| 16 | 3.52E-10         | 1.14E-10    |
| 32 | 1.73E-11         | 5.99E-12    |

## Timoshenko beam: Loss of exponential accuracy

| $N_x * N_y$ | $Q_x * Q_y$ | $u$ error | $v$ error | $\sigma_x$ error | $\tau_{xy}$ error |
|-------------|-------------|-----------|-----------|------------------|-------------------|
| 2*2         | 5*5         | 5.22E-3   | 4.90E-3   | 1.33E-2          | 2.39E-2           |
|             | 10*10       | 1.55E-4   | 5.25E-5   | 1.44E-4          | 1.02E-4           |
|             | 20*20       | 6.36E-4   | 3.47E-4   | 6.55E-4          | 7.26E-4           |
|             | 40*40       | 1.76E-3   | 1.64E-3   | 1.93E-3          | 2.57E-3           |
| 4*4         | 5*5         | 8.50E-2   | 4.04E-2   | 7.72E-2          | 4.19E-2           |
|             | 10*10       | 1.32E-5   | 6.19E-6   | 3.25E-5          | 4.22E-5           |
|             | 20*20       | 1.33E-3   | 1.12E-3   | 1.31E-3          | 1.04E-3           |
|             | 40*40       | 6.42E-4   | 1.91E-4   | 1.18E-3          | 1.38E-3           |

## Comparison with Spectral Element Method

| Local ELM                | SEM               |
|--------------------------|-------------------|
| Strong form              | Weak form         |
| Domain decomposition     | Mesh generation   |
| Extreme learning machine | Polynomial        |
| $M \neq N$               | $M = N$           |
| Spectral accuracy        | Spectral accuracy |
| Geometry more friendly   | Geometry friendly |
| Basis do not satisfy BC  | Basis satisfy BC  |

Local ELM does not work well for anisotropy/elasticity problems

# Accuracy vs Efficiency

Is there a way to combine the advantages of traditional and machine learning-based methods?

# The Random Feature Method (RFM)<sup>7</sup>

- ▶ Strong form: collocation points
- ▶ Approximation space: random feature functions
  - 1 Partition of unity and local random feature models
  - 2 Multi-scale basis
  - 3 Adaptive basis
- ▶ Soft boundary condition: Basis functions do not satisfy BC
- ▶ A linear convex optimization problem with easy-tuning parameters (balance the contributions from the PDE terms and the boundary conditions in the loss function)
- ▶  $M \neq N$

Simple, mesh-free, spectral accuracy, easy to handle complex geometries and boundary conditions

# Loss function

Examples include the elliptic problem, the linear elasticity problem, and the Stokes flow problem when  $d \leq 3$

$$\begin{cases} \mathcal{L}\mathbf{u}(\mathbf{x}) = \mathbf{f}(\mathbf{x}) & \mathbf{x} \in \Omega, \\ \mathcal{B}\mathbf{u}(\mathbf{x}) = \mathbf{g}(\mathbf{x}) & \mathbf{x} \in \partial\Omega, \end{cases}$$

where  $\mathbf{x} = (x_1, \dots, x_d)^T$ , and  $\Omega$  is bounded and connected domain in  $\mathbb{R}^d$

$$\text{Loss} = \sum_{\mathbf{x}_i \in C_I} \sum_{k=1}^{K_I} \lambda_{I_i}^k \|\mathcal{L}^k \mathbf{u}(\mathbf{x}_i) - \mathbf{f}^k(\mathbf{x}_i)\|_{l^2}^2 + \sum_{\mathbf{x}_j \in C_B} \sum_{\ell=1}^{K_B} \lambda_{B_j}^\ell \|\mathcal{B}^\ell \mathbf{u}(\mathbf{x}_j) - \mathbf{g}^\ell(\mathbf{x}_j)\|_{l^2}^2$$

Different penalty parameters at different collocation points are allowed

# Collocation points

Two sets of collocation points:  $C_I$  in  $\Omega$  and  $C_B$  on  $\partial\Omega$

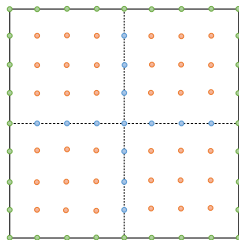


**Figure:** Collocation points for a square domain:  $C_I$ , interior points in orange and blue;  $C_B$ , boundary points in green.

# Approximation space

A linear combination of  $M$  network basis functions  $\{\phi_m\}$  over  $\Omega$  as

$$u_M(\mathbf{x}) = \sum_{m=1}^M u_m \phi_m(\mathbf{x})$$

$$\phi_m(\mathbf{x}) = \sigma(\mathbf{k}_m \cdot \mathbf{x} + b_m)$$

where  $\sigma$  is some scalar nonlinear function,  $\mathbf{k}_m, b_m$  are some random but fixed parameters



# Partition of unity

A set of points  $\{\mathbf{x}_n\}_{n=1}^{M_p} \subset \Omega$  with  $\mathbf{x}_n$  the center for a component in the partition

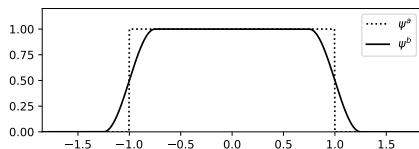


Figure: Visualization of  $\psi^a(x)$  and  $\psi^b(x)$ .

High-dimensional PoU:  $\psi_n(\mathbf{x}) = \prod_{k=1}^d \psi_n(x_k)$

## Local random feature functions

$$\tilde{\mathbf{x}} = \frac{1}{\mathbf{r}_n}(\mathbf{x} - \mathbf{x}_n), \quad n = 1, \dots, M_p$$

where  $\mathbf{r}_n = (r_{n1}, r_{n2}, \dots, r_{nd})$  and  $\{\mathbf{r}_n\}$  are preselected

- ▶ Construct  $J_n$  random feature functions by

$$\phi_{nj}(\mathbf{x}) = \sigma(\mathbf{k}_{nj} \cdot \tilde{\mathbf{x}} + b_{nj}), \quad j = 1, \dots, J_n$$

where the feature vectors  $\{(\mathbf{k}_{nj}, b_{nj})\}$  are often chosen randomly, such as  $\mathbf{k}_{nj} \sim \mathbb{U}([-R_{nj}, R_{nj}]^d)$  and  $b_{nj} \sim \mathbb{U}([-R_{nj}, R_{nj}])$

- ▶ Approximate solution

$$u_M(\mathbf{x}) = \sum_{n=1}^{M_p} \psi_n(\mathbf{x}) \sum_{j=1}^{J_n} u_{nj} \phi_{nj}(\mathbf{x})$$

Multi-scale basis

$$u_M(\mathbf{x}) = u_g(\mathbf{x}) + \sum_{n=1}^{M_p} \psi_n(\mathbf{x}) \sum_{j=1}^{J_n} u_{nj} \phi_{nj}(\mathbf{x})$$

where  $u_g$  is a global random feature function

## Adaptive basis

- ▶ Some (incomplete) information about the spectral distribution of the solution in the precomputing stage
- ▶ A spectral analysis of the forcing term for example
- ▶ Selection of the spectral distribution of the feature vectors
- ▶ Particularly useful when **sin/cos** is used as the activation function

# Optimization: A least-squares problem

Parameter tuning is fully automatic!!!

Penalty coefficients in the loss functions are chosen as

$$\lambda_{li}^k = \frac{c}{\max_{1 \leq n \leq M_p} \max_{1 \leq j' \leq J_n} \max_{1 \leq k' \leq K_l} |\mathcal{L}^{k'}(\phi_{nj'}^{k'}(\mathbf{x}_i)\psi_n(\mathbf{x}_i))|} \quad \mathbf{x}_i \in C_l, k = 1, \dots, K_l$$

$$\lambda_{Bj}^\ell = \frac{c}{\max_{1 \leq n \leq M_p} \max_{1 \leq j' \leq J_n} \max_{1 \leq \ell' \leq K_l} |\mathcal{B}^{\ell'}(\phi_{nj'}^{\ell'}(\mathbf{x}_j)\psi_n(\mathbf{x}_j))|} \quad \mathbf{x}_j \in C_B, \ell = 1, \dots, K_B$$

where  $c = 100$  is a universal constant

# Collocation points

- ▶ Explicit representation of boundary
  - Uniform grid over the computational domain
  - Uniform grid in the parameter space
- ▶ Implicit representation of boundary
  - Easily identify interior points
  - Define an energy function for finding a point on the boundary

# Numerical setup

- ▶ Select a set of points  $\{\mathbf{x}_n\}_{n=1}^{M_p}$  and construct the PoU
- ▶ Construct  $J_n$  random feature functions with radius  $r_n$  for each  $\mathbf{x}_n$
- ▶ Sample  $Q$  collocation points
- ▶ Total number of random feature functions  $M$
- ▶ Total number of conditions  $N$
- ▶ Typically  $N > M$  due to the geometric complexity and the limited computational resource

# Partition of unity and local random feature models

Table: Comparison of the RFM and PINN for the one-dimensional Helmholtz equation

| M    | $\psi^a$ |                  | $\psi^b$ |                  | PINN |                  |
|------|----------|------------------|----------|------------------|------|------------------|
|      | N        | $L^\infty$ error | N        | $L^\infty$ error | N    | $L^\infty$ error |
| 200  | 208      | 8.76E-2          | 202      | 2.51E-2          | 202  | 2.59E-2          |
| 400  | 416      | 5.89E-7          | 402      | 5.18E-7          | 402  | 6.77E-3          |
| 800  | 832      | 4.44E-10         | 802      | 6.61E-10         | 802  | 1.35E-2          |
| 1600 | 1664     | 8.84E-12         | 1602     | 1.18E-11         | 1602 | 8.94E-3          |

- ▶ Error in PINN is around  $1E-3$  without notable further improvement ← Optimization error
- ▶ RFM for different PoU functions has exponential convergence ← representability of random feature functions
- ▶ RFM has exponential convergence for all problems tested when  $d = 1, 2, 3$



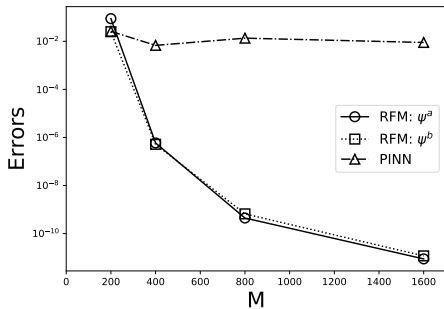
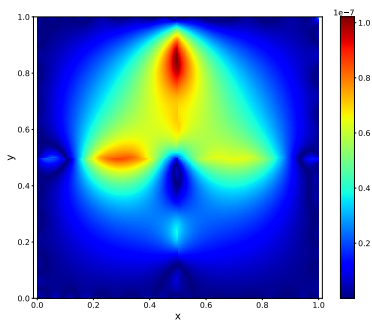
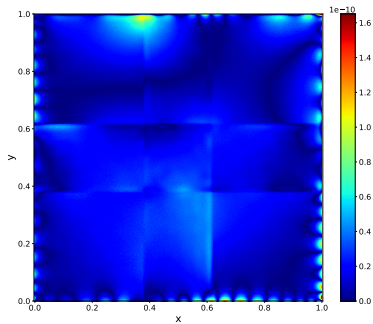


Figure: Convergence of RFM and PINN for Helmholtz equation in the semi-log scale

# Different choice of PoU



(a)  $\psi^a$



(b)  $\psi^b$

**Figure:** Error distribution of the RFM with different choices of PoU for Poisson equation

# Multi-scale basis

**Table:** Comparison of PoU-based local basis and multi-scale basis functions for Poisson equation with the explicit solution

| Solution frequency | M    | N    | PoU-based basis | Multi-scale basis |
|--------------------|------|------|-----------------|-------------------|
| Low                | 1200 | 1920 | 1.93E-8         | 3.28E-9           |
|                    | 2700 | 4320 | 3.62E-9         | 6.42E-10          |
|                    | 4800 | 7680 | 8.61E-10        | 3.05E-10          |
| High               | 1200 | 1920 | 6.42E-6         | 9.36E-7           |
|                    | 2700 | 4320 | 1.34E-7         | 3.58E-8           |
|                    | 4800 | 7680 | 4.16E-8         | 1.75E-8           |
| Mixed              | 1200 | 1920 | 3.22E-6         | 4.68E-7           |
|                    | 2700 | 4320 | 6.54E-8         | 1.80E-8           |
|                    | 4800 | 7680 | 2.06E-8         | 8.92E-9           |

Inclusion of global basis functions improves the accuracy when the solution has a significant low-frequency component

## Adaptive basis

Table: Results of using adaptive random feature functions for the two-dimensional Poisson equation

| $R_m$ | tanh                    |                | sin                     |                |
|-------|-------------------------|----------------|-------------------------|----------------|
|       | $\mathbb{U}[-R_m, R_m]$ | Equally spaced | $\mathbb{U}[-R_m, R_m]$ | Equally spaced |
| 0.5   | 4.92E-9                 | 1.01E-9        | 2.55E-3                 | 6.05E-4        |
| 1.0   | 2.91E-8                 | 9.36E-9        | 8.96E-7                 | 2.58E-5        |
| 1.5   | 1.33E-6                 | 5.95E-7        | 1.79E-9                 | 1.47E-6        |
| 2.0   | 8.75E-5                 | 7.85E-5        | 3.30E-12                | 4.29E-7        |
| 2.5   | 8.16E-4                 | 4.70E-5        | 2.86E-12                | 7.66E-6        |
| 3.0   | 2.06E-2                 | 5.27E-4        | 7.32E-12                | 2.17E-5        |
| 3.5   | 1.53E-3                 | 3.95E-3        | 6.10E-12                | 7.45E-5        |
| 4.0   | 2.66E-3                 | 1.27E-3        | 6.10E-12                | 5.59E-5        |
| 4.5   | 5.39E-3                 | 1.76E-2        | 2.29E-11                | 1.24E-3        |
| 5.0   | 1.29E-2                 | 5.16E-2        | 2.17E-11                | 6.72E-3        |

Best results: **sin** activation function with  $R_m \geq k$  and random initialization

# Timoshenko beam problem: Elasticity problem in two dimension

Table: Comparison of RFM and locELM

| Method | $M$ | $N$   | $u$ error | $v$ error | $\sigma_x$ error | $\tau_{xy}$ error |
|--------|-----|-------|-----------|-----------|------------------|-------------------|
| RFM    | 800 | 400   | 1.36E-2   | 3.43E-3   | 1.40E-2          | 1.63E-2           |
|        |     | 1200  | 7.14E-6   | 7.98E-7   | 8.93E-6          | 7.45E-6           |
|        |     | 4000  | 6.41E-11  | 4.34E-11  | 6.41E-11         | 6.58E-11          |
|        |     | 14400 | 8.16E-12  | 1.01E-12  | 1.07E-11         | 1.03E-11          |
| locELM | 800 | 400   | 5.22E-3   | 4.90E-3   | 1.33E-2          | 2.39E-2           |
|        |     | 1200  | 1.55E-4   | 5.25E-5   | 1.44E-4          | 1.02E-4           |
|        |     | 4000  | 6.36E-4   | 3.47E-4   | 6.55E-4          | 7.26E-4           |
|        |     | 14400 | 1.76E-3   | 1.64E-3   | 1.93E-3          | 2.57E-3           |

Rescaling strategy restores the spectral accuracy

## Two-dimensional elasticity problem with a complex geometry

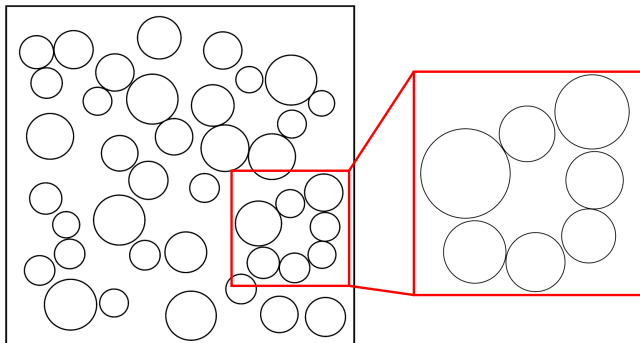
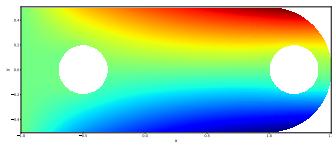


Figure: Complex domain with a cluster of holes that are nearly touching

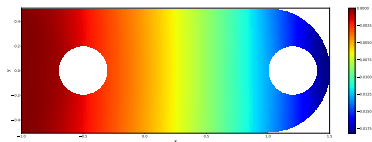
# Rescaling

Error in locELM is around  $10^{-3} \sim 10^{-2}$ , while RFM still maintains spectral accuracy

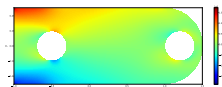
| $M$   | $N$    | $u$ error | $v$ error | $\sigma_x$ error | $\sigma_y$ error | $\tau_{xy}$ error |
|-------|--------|-----------|-----------|------------------|------------------|-------------------|
| 3200  | 1784   | 4.96E-1   | 8.37E-1   | 1.09E+0          | 3.52E+0          | 5.24E-1           |
|       | 4658   | 5.82E-3   | 7.12E-3   | 1.04E-2          | 5.47E-2          | 3.85E-3           |
|       | 13338  | 1.69E-5   | 1.19E-5   | 2.89E-5          | 6.40E-5          | 8.18E-6           |
|       | 42820  | 1.39E-5   | 1.55E-5   | 4.92E-5          | 6.16E-5          | 1.29E-5           |
| 12800 | 6578   | 9.11E-2   | 6.41E-2   | 1.03E-1          | 2.46E-1          | 2.95E-2           |
|       | 17178  | 2.35E-4   | 2.10E-4   | 3.02E-4          | 7.56E-4          | 8.93E-5           |
|       | 50500  | 5.46E-7   | 4.98E-7   | 8.45E-7          | 2.03E-6          | 2.67E-7           |
|       | 165184 | 2.32E-7   | 1.89E-7   | 9.28E-8          | 2.32E-7          | 2.43E-8           |



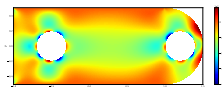
(a)  $u$



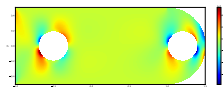
(b)  $v$



(c)  $\sigma_x$



(d)  $\tau_{xy}$



(e)  $\sigma_y$

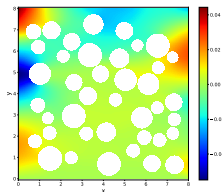
Figure: Numerical solution by the random feature method for the elasticity problem



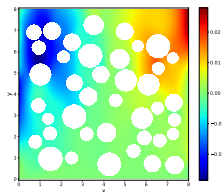
Difference between the RFM and FEM solutions is about 1%

| Method | Reference        | $M$   | $N$    | $u$ error | $v$ error | $\sigma_x$ error | $\sigma_y$ error | $\tau_{xy}$ error |
|--------|------------------|-------|--------|-----------|-----------|------------------|------------------|-------------------|
| RFM    | RFM $N = 490176$ | 16000 | 40326  | 1.28E+0   | 1.12E+0   | 1.29E+0          | 9.37E-1          | 1.03E+0           |
|        |                  |       | 135442 | 1.12E-1   | 1.16E-1   | 1.13E-1          | 1.03E-2          | 1.20E-1           |
|        |                  |       | 285472 | 6.52E-4   | 6.98E-4   | 1.03E-3          | 3.01E-5          | 1.88E-3           |
| RFM    | FEM $M = 153562$ | 16000 | 40326  | 1.30E+0   | 1.12E+0   | 1.28E+0          | 9.37E-1          | 1.03E+0           |
|        |                  |       | 135442 | 7.65E-2   | 8.55E-2   | 1.16E-1          | 1.31E-1          | 1.25E-1           |
|        |                  |       | 285472 | 3.94E-2   | 3.36E-2   | 6.59E-3          | 5.95E-2          | 2.31E-2           |
| FEM    | FEM $M = 153562$ | 16000 | 490176 | 4.00E-2   | 3.43E-2   | 6.20E-3          | 5.92E-2          | 2.30E-2           |
|        |                  |       | 3716   | 3.15E-4   | 4.54E-4   | 1.41E-2          | 5.81E-2          | 3.35E-2           |
|        |                  |       | 10438  | 1.20E-4   | 1.81E-4   | 9.39E-3          | 3.61E-2          | 2.13E-2           |
| FEM    | FEM $M = 153562$ | 16000 | 10438  | 2.88E-5   | 3.93E-5   | 4.65E-3          | 1.62E-2          | 9.40E-3           |
|        |                  |       | 40054  | 2.88E-5   | 3.93E-5   | 4.65E-3          | 1.62E-2          | 9.40E-3           |
|        |                  |       | 40054  | 2.88E-5   | 3.93E-5   | 4.65E-3          | 1.62E-2          | 9.40E-3           |
| FEM    | RFM $N = 490176$ | 16000 | 3716   | 3.87E-2   | 3.36E-2   | 1.43E-2          | 8.93E-2          | 3.86E-2           |
|        |                  |       | 10438  | 3.86E-2   | 3.34E-2   | 1.05E-2          | 7.29E-2          | 2.99E-2           |
|        |                  |       | 40054  | 3.85E-2   | 3.32E-2   | 7.19E-3          | 6.33E-2          | 2.44E-2           |
| FEM    | RFM $N = 490176$ | 16000 | 153562 | 3.85E-2   | 3.32E-2   | 6.22E-3          | 6.01E-2          | 2.31E-2           |
|        |                  |       | 153562 | 3.85E-2   | 3.32E-2   | 6.22E-3          | 6.01E-2          | 2.31E-2           |

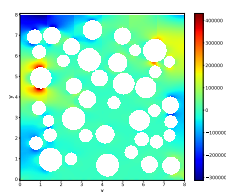
Table: Comparison of RFM and FEM



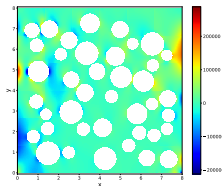
(a)  $u$



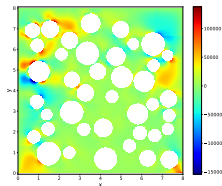
(b)  $v$



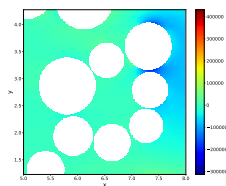
(c)  $\sigma_x$



(d)  $\sigma_y$



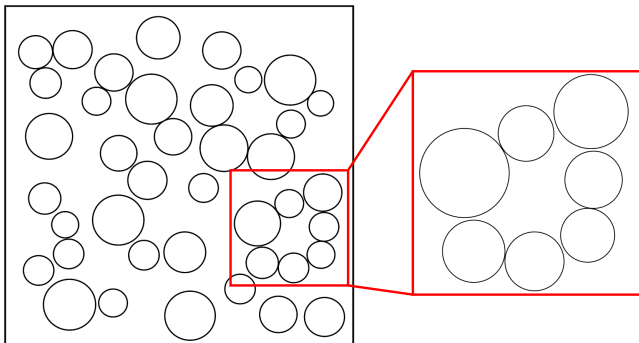
(e)  $\tau_{xy}$



(f)  $\sigma_x$  over a cluster

Figure: Numerical solution by the random feature method for the two-dimensional elasticity problem over a complex geometry

## Mesh generation in FEM is difficult

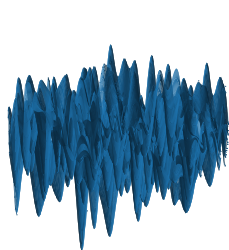


Removal of the cluster leads to an  $L^\infty$  error of about 50% for  $\sigma_x$   
RFM shows a clear trend of numerical convergence

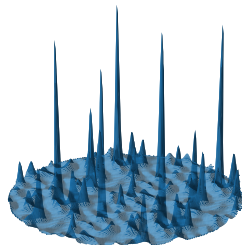
| $M$   | $N$    | $u$ error | $v$ error | $\sigma_x$ error | $\sigma_y$ error | $\tau_{xy}$ error |
|-------|--------|-----------|-----------|------------------|------------------|-------------------|
| 14400 | 195146 | 2.30E-1   | 1.30E-1   | 6.64E-2          | 1.72E-1          | 1.71E-1           |
|       | 226132 | 8.97E-2   | 1.23E-1   | 5.60E-2          | 1.41E-1          | 1.32E-1           |
|       | 259400 | 6.47E-2   | 6.94E-2   | 3.66E-2          | 9.04E-2          | 8.15E-2           |
|       | 294878 | 7.30E-2   | 6.68E-2   | 3.46E-2          | 7.13E-2          | 7.05E-2           |

Table: Numerical results of the RFM with  $N = 332606$  as the reference

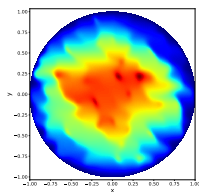
# Multi-scale problems



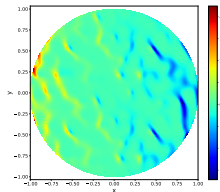
(a)  $h$



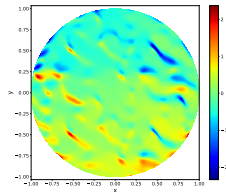
(b)  $a$



(c)  $u$



(d)  $u_x$



(e)  $u_y$

Figure: Random feature method for the elliptic homogenization problem

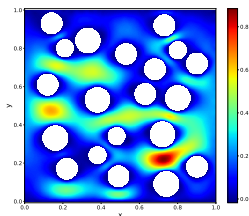
Table: Convergence of RFM

| $M$   | $N$    | $u$ error | $u_x$ error | $u_y$ error |
|-------|--------|-----------|-------------|-------------|
| 25600 | 25554  | 1.42E+0   | 8.68E+0     | 8.73E+0     |
|       | 91339  | 3.13E-2   | 3.54E-2     | 3.62E-2     |
|       | 197360 | 3.48E-3   | 6.45E-3     | 7.18E-3     |
|       | 343586 |           | Reference   |             |

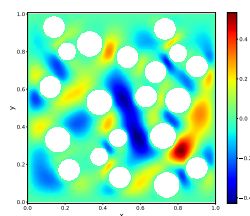
# Stokes flow

Two-dimensional channel flows with the inhomogeneous boundary condition

$$(u, v)|_{\partial\Omega} = \begin{cases} (y(1-y), 0) & \text{if } x = 0 \\ (y(1-y), 0) & \text{if } x = 1 \\ (0, 0) & \text{otherwise} \end{cases}$$



(a)  $u$

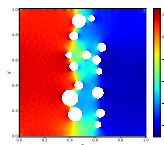


(b)  $v$

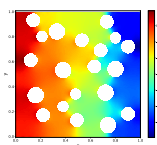
Figure: Velocity field  $(u, v)$  generated by the random feature method

# Pressure diagram for four sets of complex obstacles

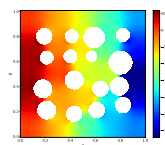
- ▶ Spurious pressure mode arises due to the rank deficiency of the discrete systems in spectral methods  $M = N^8$
- ▶ RFM automatically bypass this issue by looking for the minimal-norm solution  $M \neq N$



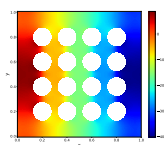
(a)



(b)



(c)



(d)

# Discussions

## Three key components of RFM

- 1 Loss function: least-squares (strong) formulation of the PDEs on collocation points
  - 2 Approximate solution: linear combination of random feature functions
  - 3 Optimization: least-squares problem with automatic parameter tuning
- ▶ Traditional algorithms are robust but lack of flexibility
  - ▶ Machine-learning algorithms are flexible but lack of robustness
  - ▶ RFM seems to have both



- ▶ Deep neural networks have strong representative power but the parameters are difficult to optimize
- ▶ Random feature functions seem to also have strong representative power and the parameters are “easy” to optimize
- ▶ Classical methods  $M = N$ : Efficient linear solvers
- ▶ Random feature method  $M \neq N$ : Least square framework with large condition number

## Further developments

- ▶ Choice of basis functions: Probability distribution for the feature vector
- ▶ Choice of collocation points: Three dimensional domains when the boundary is a surface
- ▶ Training: Preconditioning and reformulation techniques
- ▶ Time-dependent problems
- ▶ Applications